# SYMBIODINIUM NATANS SP. NOV.: A ''FREE-LIVING'' DINOFLAGELLATE FROM TENERIFE (NORTHEAST-ATLANTIC OCEAN)[1]

## Gert Hansen[2] and Niels Daugbjerg

Department of Biology, Phycology Laboratory, University of Copenhagen, Øster Farimagsgade 2D,
DK-1353 Copenhagen K., Denmark

We examined a free-living *Symbiodinium* species by light and electron microscopy and nuclear-encoded partial LSU rDNA sequence data. The strain was isolated from a net plankton sample collected in near-shore waters at Tenerife, the Canary Islands. Comparing the thecal plate tabulation of the free-living *Symbiodinium* to that of *S. microadriaticum* Freud., it became clear that a few but significant differences could be noted. The isolate possessed two rather than three antapical plates, six rather than seven to eight postcingular plates, and finally four rather than five apical plates. The electron microscopic study also revealed the presence of an eyespot with brick-shaped contents in the sulcal region and a narrow anterior plate with small knob-like structures. Bayesian analysis revealed the free-living *Symbiodinium* to be a member of the earliest diverging clade A. However, it did not group within subclade $A_I$ (=temperate A) or any other subclades within clade A. Rather, it occupied an isolated position, and this was also supported by sequence divergence estimates. On the basis of comparative analysis of the thecal plate tabulation and the inferred phylogeny, we propose that the *Symbiodinium* isolate from Tenerife is a new species (viz. *S. natans*). To elucidate further the species diversity of *Symbiodinium*, particularly those inhabiting coral reefs, we suggest combining morphological features of the thecal plate pattern with gene sequence data. Indeed, future examination of motile stages originating from symbiont isolates will demonstrate if this proves a feasible way to identify and characterize additional species of *Symbiodinium* and thus match ribotypes or clusters of ribotypes to species.

*Key index words:* free-living *Symbiodinium*; LSU rDNA; molecular phylogeny; plate tabulation; ultrastructure

*Abbreviations:* BA, Bayesian analysis; ITS, internal transcribed spacer; LB, longitudinal basal body; LSC, longitudinal striated collar; NJ, neighbor joining; src, striated root connective; TB, transverse basal body; TMRE, transverse microtubular root extension; TSC, transverse striated collar; vc, ventral connective

The term zooxanthellae refers to the golden-brown-colored algae living in mutualistic symbiosis with various invertebrate and protist hosts. Although they may include cryptophytes and diatoms, dinoflagellates constitute by far the most common group (Trench and Blank 1987, Rowan 1998). Earlier studies suggested that the endosymbionts represented a single pandemic dinoflagellate species, *Symbiodinium microadriaticum* (McLaughlin and Zahl 1966), but the advent of ultrastructural, biochemical, and later molecular systematics suggested the presence of different *Symbiodinium* species, and even dinoflagellate species from other genera, for example, *Amphidinium, Aureodinium, Gloeodinium, Gymnodinium,* and *Scrippsiella* (Trench 1987, Wakefield et al. 2000). Still, species of *Symbiodinium* are the most widespread types of endosymbionts and have been found, besides cnidarians, in such diverse groups as foraminiferans, radiolarians, ciliates, mollusks, and sponges (Baker 2003). The genus comprises four validly described species (*S. microadriaticum, S. pilosum* Trench et R. J. Blank ex. Trench, *S. kawagutii* Trench et R. J. Blank ex. Trench, and *S. goreauii* Trench et R. J. Blank ex. Trench) and seven species without a formal description (*S. bermudense, S. californicum, S. cariborum, S. corculorum, S. meandrinae, S. muscatinei,* and *S. pulchrorum*) (Banaszak et al. 1993, LaJeunesse and Trench 2000). Additionally, nuclear-encoded LSU gene of *Gymnodinium linucheae* (Trench et Thinh) has ≥98% sequence similarity with *S. microadriaticum* and also belongs to *Symbiodinium* (Wilcox 1998). The correct combination was made by LaJeunesse (2001) as *S. linucheae* (Trench et Thinh) LaJeunesse. *Gymnodinium beii* Spero and the CCMP 1321 strain referred to as *Gymnodinium simplex* (Lohmann) Kofoid et Swezy are also closely related to *Symbiodinium,* and a free-living strain from New Zealand referred to as ''*Gymnodinium varians*'' Maskell has turned out to be a misidentified *Symbiodinium* species. All three species share a large deletion in the D2 region of the LSU gene

---

with *Symbiodinium* (Wilcox 1998). Hence, the genus *Gymnodinium* might be removed from the list of zooxanthellae. The genus *Aureodinium* also seems to be closely related to *Symbiodinium.* They share several characters, for example, the presence of numerous polygonal plates, a stalked pyrenoid, lack of trichocysts, and a coccoid phase in the life history (Dodge 1967).

The molecular phylogenies, based on noncoding (ITS 1 and ITS 2) or coding (5.8S, SSU, LSU rDNA, cp23S rDNA) DNA fragments and also concatenated analyses, have consistently divided the genus into originally three but at present eight clades, designated A to H (Rowan and Powers 1992, Carlos et al. 1999, LaJeunesse 2001, Santos et al. 2002, Baker 2003, Garcia-Cuetos et al. 2005, Pochon et al. 2006). Some of the clades are further subdivided into subclades and numerous molecular ''types'' representing terminal taxa. About 100 types have been identified so far (Baker 2003), but uncertainty still exists concerning the taxonomic level these types represent (i.e., species, variants, populations, or clonal strains). Often the genetic difference between types is considerably larger than between species or even orders in other dinoflagellate groups (Baker 2003, Coffroth and Santos 2005). Formal descriptions are hampered by the scanty morphological features of the coccoid stage, and details of the motile cells are rarely included (Loeblich and Sherley 1979). Characters used to circumscribe species include size of the coccoid and motile stages, number and volume of chromosomes, number of chloroplasts and pyrenoid stalks, thylakoid arrangement, and also isoelectrical characteristics of peridinin–chl *a*–protein complexes (PCP) (Trench and Blank 1987).

Plate tabulation characteristics are the primary foundation for the taxonomy of armored dinoflagellates (Balech 1980, Fensome et al. 1993), but detailed analyses of the thecal plate pattern of the motile stage of *Symbiodinium* have so far only been performed for *S. microadriaticum* (Loeblich and Sherley 1979). Trench and Blank (1987) observed differences in plate patterns of *S. microadriaticum, S. pilosum, S. kawagutii,* and *S. goreauii* but did not provide any details. Thus, plate tabulation of *Symbiodinium* spp. could be a potential useful feature as a taxonomic criterion for species identification.

In the present study, we provide detailed plate analyses and include an ultrastructural characterization of a *Symbiodinium* species isolated from the water column in nearshore waters of Tenerife in the northeast Atlantic Ocean. The plate pattern was different from *S. microadriaticum,* and its phylogenetic positions within clade A based on partial LSU rDNA sequences also suggested it as a new species. We propose to name it *Symbiodinium natans* Gert Hansen et Daugbjerg sp. nov.

## MATERIALS AND METHODS

The clonal culture used in this study was established from a net sample (20 μm mesh size, Aquanet, Kastrup, Denmark) collected from a pier at Callao Salvaje, Tenerife (28°7′36″N, 16°46′56″E), October 2004. The sample was enriched with TL growth medium (Larsen et al. 1994) and incubated at 20°C for about a week. Single cells of potentially interesting small dinoflagellates were isolated using a micropipette and a Labovert inverted microscope (Leitz, Wetzlar, Germany). The *Symbiodinium* culture used in the present study was grown in TL medium, at 20°C and ∼40 μmol · m$^{-2}$ · s$^{-1}$. The culture was maintained for nearly 3 years before a culture cabinet failure unfortunately ended its growth.

*LM.* LM of live cells was made using an Provis AX 70 (Olympus, Tokyo, Japan) with a 60× dry lens, N.A. 0.90. Microphotography was made using a Axiocam HR digital camera (Zeiss, Jena, Germany).

*SEM.* Cells were fixed in 2% OsO$_4$ for either 3 min or 40 min and placed on poly-L-lysine coated circular coverslips or polycarbonate filters of 5 μm pore size (Isopore, Millipore Corp., Bedford, MA, USA). After washing in dH$_2$O for 1 h, samples were dehydrated in an ethanol series: 30, 50, 70, 96, and 99.9% for 10 min in each change, and finally in two changes of 100% ethanol, 30 min in each change. Critical-point drying was in a BAL-TEC CPD-030 (Balzers, Liechtenstein). The filters or coverslips were mounted on stubs and coated with palladium-platinum and examined in a JEOL JSM-6335F field emission scanning electron microscope (JEOL, Tokyo, Japan).

*TEM.* One vol. culture was added to one vol. fixation cocktail consisting of 2% glutaraldehyde made up in 0.2 M Na-cacodylate buffer with 0.3 M sucrose. The culture was pelleted by centrifugation after 1 h fixation and washed in four changes of buffer with decreasing sucrose concentration: 0.3 M, 0.15 M, 0.075 M, and straight 0.1 M buffer, 20 min in each change.

Postfixation was 1 h in 2% OsO$_4$ made up in 0.1 M Na-cacodylate buffer, and the material was dehydrated in an ethanol series and embedded in Spurr's resin via propylene oxide. The material was sectioned on a Reichert Ultracut E ultramicrotome (Leica, Wetzlar, Germany) using a diamond knife. The sections were collected on slot grids and placed on formvar film. After staining in uranyl acetate and lead citrate, sections were examined in a JEOL JEM-1010 electron microscope operated at 80 kV. Micrographs were taken using a GATAN 792 digital camera (GATAN, Pleasanton, CA, USA).

Several, more or less successful, fixation schedules were applied. The schedule outlined above provided acceptable preservation of the internal parts of the cell but also pronounced osmotic artifacts of the amphiesma (i.e., thecal plates could not be recognized, and both flagella were lost).

*DNA extraction, PCR amplification, and LSU rDNA sequencing.* Ten mL of a clonal culture of *S. natans* was harvested by centrifugation at 3,000*g* for 10 min. The resulting pellet was transferred to a 1.5 mL Eppendorf tube and placed at −20°C for ∼2 weeks. Following thawing of the cell pellet, total genomic DNA was extracted using the CTAB (hexadecyltrimethyl-ammonium bromide) protocol as previously outlined (Daugbjerg et al. 1994). Amplification of partial nuclear-encoded LSU rDNA by the use of PCR was performed in a 50 μL reaction containing 5 μL 10X Taq buffer (67 mM Tris-HCl, pH 8.5, 2 mM MgCl$_2$, 16.6 mM (NH$_4$)$_2$SO$_4$ and 10 mM β-mercaptoethanol), 20 μL 0.5 μM dNTP mix, 5 μL 10 μM of each primer, 5 μL 100 mM tetramethylammonium chloride (TMA), and 1 U Taq polymerase (Ampliqon, Herlev, Denmark). The amplification primers were D1R-F (forward primer) combined with 28-1483 (reverse primer). Primer sequences are given in Scholin et al. (1994) and Daugbjerg et al. (2000), respectively. The PCR temperature profile was

one initial cycle of denaturation at 94°C. This step was followed by 35 cycles where each cycle comprised the following steps: denaturation at 94°C for 1 min, annealing at 52°C for 1 min, and extension at 72°C for 3 min. The temperature profile was ended with a final extension step at 72°C for 6 min. The copies of LSU rDNA fragments were loaded into a 2% NuSieve gel containing ethidium bromide. After running the gel for 15 min at 150 volts, it was placed on a UV light table. A molecular marker (Phi X175 HAE III) was used to ensure that the PCR fragments had the anticipated length. PCR fragments were purified using the QIAquick PCR purification kit, and for sequence determination, 30 nanograms of DNA was added to a total reaction volume of 20 μL. The nucleotide sequence was determined using the dye terminator cycle sequencing ready reaction kit (Perkin Elmer, Foster City, CA, USA) as suggested by the manufacturer. Sequencing reactions were loaded on an ABI PRISM 377 DNA sequencer (Perkin Elmer), and partial LSU rDNA was determined in both directions using the two amplification primers in addition to the following internal primers D3A and D3B (Nunn et al. 1996) and D2C (Scholin et al. 1994).

*Alignment and phylogenetic analyses.* The alignment used to infer the phylogeny of the free-living culture of *Symbiodinium* from Tenerife was kindly provided by Lydia Garcia-Cuetos and is therefore identical to the data matrix applied in Garcia-Cuetos et al. (2005). However, prior to our analyses, we modified it to include only nuclear-encoded LSU rDNA sequences and furthermore added 30 additional *Symbiodinium* sequences available in GenBank, representing clade A with 12 sequences, clade B with 12 sequences, and clade D with six sequences. The final alignment including the isolate from Tenerife comprised 106 *Symbiodinium* sequences and a total of 815 base pairs including introduced gaps. Two outgroup taxa *Gymnodinium beii* and *G. simplex* were used to polarize the ingroup of *Symbiodinium,* based on a study by Gast and Caron (1996) showing that these two dinoflagellates were basal to *Symbiodinium.* The alignment was manually edited with MacClade (ver. 4.08, Maddison and Maddison 2003), and the resulting data matrix was analyzed using Bayesian (MrBayes ver. 3.1.2, Ronquist and Huelsenbeck 2003) and neighborjoining (NJ) methods. Bayesian analysis (BA) was performed using a GRT (general time reversible) substitution model with base frequencies and substitution rate matrix estimated from the data. In total $2*10^6$ Markov Chain Monte Carlo (MCMC) generations with four parallel chains (three heated and one cold) were performed. A tree was sampled every 50th generation. According to AWTY (Are We There Yet) by Wilgenbusch et al. (2004) the BA (with $2*10^6$ generations) had been running long enough as the plots of posterior probabilities of all splits for paired MCMC runs converged using the compare command (data not shown). Plotting the log likelihood values as a function of generations in MS Excel (Microsoft Corp., Seattle, WA, USA), the lnL values converged at ~6,885 after 60,000 generations. We used this number of generations as the burn-in, resulting in 38,801 trees that were imported into PAUP* (ver. 4b10, Swofford 2003) and a 50% majority-rule consensus tree was constructed. Prior to the phylogenetic analysis based on NJ we invoked Modeltest (ver. 3.7, Posada and Crandall 1998) to find the best-fit model for the partial LSU rDNA gene sequences by hierarchical likelihood ratio tests. The model chosen was TrN+I+G (Tamura and Nei 1993) with among sites rate heterogeneity ($\alpha = 0.821$), an estimated proportion of invariable sites ($I = 0.3153$), and two substitution-rate categories (A-G = 4.2632 and C-T = 8.413). Base frequencies were set as follows: A = 0.2456, C = 0.1883, G = 0.2962, and T = 0.2699. This model was applied to compute dissimilarity values, and we used the resulting distance matrix to build a tree with the NJ method using PAUP*. NJ bootstrapping invoked 1,000 replications.

## RESULTS

***Symbiodinium natans*** sp. nov. Gert Hansen et Daugbjerg.

*Description.* Cellulae mobiles circiter 10 μm longae (9.5–11.5 μm) et 8 μm latae (7.4–9 μm). Epitheca leviter latior quam hypotheca. Apicalis theca angusta elongataque plurimis cum tuberibus in apice sita. Cingulum cinguli unius latitudine dispositum. Ex duabus lineis thecarum pentagonalium constat. Thecae formula x, EAV, 4′, 5a, 8″, ?s, ?c, 6t′, 2‴′. Praesentia unius pyrenoidis duplici calamo in media cellula siti. Nucleus in epitheca situs. Stigma ex plurimis vesiculis latericii forma in sulco. Pedunculus unus praesens. GenBank accessus numerus EU315917.

Motile cells are ~10 μm long (range 9.5–11.5 μm) and 8 μm wide (range 7.4–9 μm). The episome is slightly larger than the hyposome. An apical narrow elongated amphiesmal vesicle (EAV) with numerous knobs is located at the apex. The cingulum is displaced one cingular width and consists of two rows of pentagonal plates. Plate formula: x, EAV, 4′, 5a, 8″, ?s, ?c, 6t′, 2‴′. One two-stalked pyrenoid is situated in median part of the cell. The nucleus is located in the episome. An eyespot, consisting of numerous brick-containing vesicles, is present in the sulcus. A peduncle is present. GenBank accession number: EU315917.

*Etymology: natans* referring to the free-swimming cells of this species.

*Holotype:* A SEM stub of the clonal culture used in this study has been deposited at the Botanical Museum, University of Copenhagen, accession number CAT2393. Figure 3, A–C, has been chosen to represent the type in accordance to fulfill article 39.1 of the International Code of Botanical Nomenclature (ICBN).

*Type locality:* Callao Salvaje, Tenerife.

*LM.* The typical motile cell had a slightly longer epi- than hyposome (Fig. 1A), although some variations were noted from very pronounced "mushroom-shaped" (not shown) to an almost equally sized epi- and hyposome (Fig. 1C). Brownish chloroplast(s) were situated along the cell periphery, and a distinct pyrenoid surrounded by a starch layer was located just below the nucleus (Fig. 1C). A darker brownish body, assumed to be the eyespot, was present in the sulcal area (Fig. 1, A and B). A majority of cells in the log phase were in the motile phase and had a very characteristic "spinning" movement, staying at the same place as if attached to the bottom of the culture flask, only occasionally swimming for a short distance.

The immotile cells measured ~13 μm in diameter and were often packed with storage products, particularly in old cultures (Fig. 1E). Scattered two-celled division stages were occasionally observed on the bottom of the culture flask, but four-celled stages were never recognized (Fig. 1D).
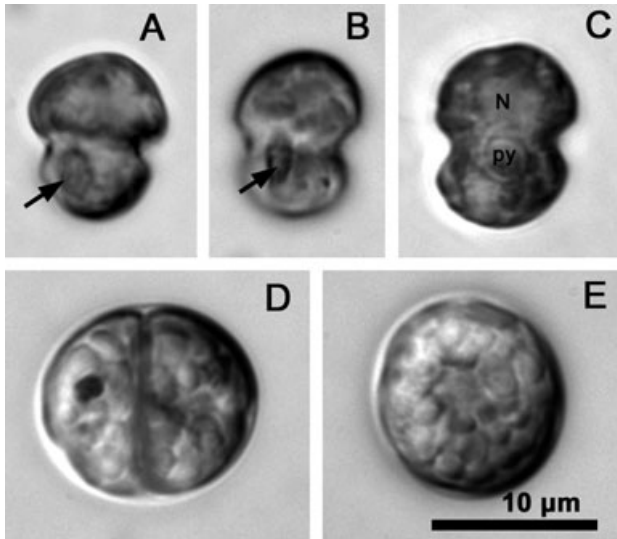
Fig. 1. *Symbiodinium natans* sp. nov., DIC LM. (A–C) Motile cells showing the putative eyespot (arrow), the nucleus (N), and the pyrenoid (py). Notice focal plane is in the cell. (D) Two-celled division cyst. (E) Immotile predivision cyst.

*SEM.* SEM revealed the transverse and longitudinal flagella, the length of the latter being more than 1.5 times the cell length (Fig. 2A). The cingular displacement was about one cingular width, and a peduncle emerged between the exit points of the two flagella (Fig. 2B).

The thecal plates were evident in many cells (Fig. 2, B–I) allowing us to reconstruct the thecal plate pattern (Fig. 3, A–C). On the episome, a narrow elongated plate or vesicle, measuring $\sim$2 μm in length and 0.2 μm in width was situated at the apex of cells (Fig. 2, F–H). We designate this plate the elongated amphiesmal vesicle (EAV) in accordance with the terminology used by Moestrup and Daugbjerg (2007). About 12 tiny knob-like structures were protruding from the EAV (Fig. 2H). A small plate (x) was associated with the ventral part of the EAV (Figs. 2, F and G; 3, A and B). Four plates, apart from the x-plate bordered the EAV. According to Kofoidean terminology, we consider these as apical plates. Plate 1′ was relatively large and rhomboid in shape, while plates 2′ and 4′ were narrow and somewhat rectangular (Fig. 2G). Eight precingular plates were present (Figs. 2, D–F; 3B), although a specimen with an extra precingular plate caused by division of plate 4″ was observed (not shown). Five plates were located between the apical and precingular series, the so-called anterior intercalary plates (Figs. 2, F and G; 3B). The hyposomal plates comprised six postcingular and two antapical plates (Figs. 2I; 3C). The cingulum was made up of numerous pentagonal plates (Figs. 2, C–E; 3A). The exact number was not determined, but judging from the SEM micrographs of cells seen at different angles, the number was

estimated to be $\sim$20. The cingular plates were arranged in two rows. The SEM fixation did not allow for a detailed analysis of the sulcal plates, but a large posterior and a narrow left sulcal plate were evident (Fig. 2C). Tiny accessory sulcal plates surrounded the flagellar pores, but their definite numbers and shapes were not evident. Two small plates, a triangular plate situated next to the 8″-plate and the plate located left anteriorly to the transverse flagellar pore, might also be interpreted as either sulcal plates or alternatively as a precingular and a cingular plate, respectively. For the time being, we have designated these as s? (Figs. 2, B and C; 3A).

*TEM. General ultrastructure:* Thin sectioning revealed the presence of numerous chloroplast profiles located along the cell periphery (Fig. 4, A and B). It is possible that these profiles represented a single chloroplast. Numerous parallel thylakoid bands arranged in groups of three were present, and three membranes surrounded the chloroplast(s) (Fig. 6G). A large pyrenoid surrounded by a distinct polysaccharide cap was situated in the central part of the cell. The pyrenoid was two-stalked, that is, attached to two of the chloroplast profiles (Fig. 4A). A typical dinoflagellate cell nucleus with condensed chromosomes, the dinokaryon, was situated in the anterior part of the cell (Fig. 4A). Mitochondrial profiles with tubular cristae, and also lipid globules were scattered throughout the cell (Fig. 4A). Pusules were associated with both the transverse and longitudinal flagellar canal (Figs. 5B; 6, A and B). They were not studied in detail but appeared to consist of a convoluted tubule. Trichocysts were never observed in the literally hundreds of cell profiles examined.

The eyespot was located in the sulcus and consisted of numerous flattened vesicles or cisternae containing electron translucent brick-shaped structures. A microtubular strand, probably the $r_1$ flagellar root was located between the eyespot and the inner amphiesmal membrane (Fig. 4C).

Unfortunately, the amphiesma could not be studied due to osmotic artifacts (Fig. 4A); for example, the thecal plates appeared to have been lost. However, plates inside the amphiesmal vesicles have previously been demonstrated in *S. microadriaticum* (Loeblich and Sherley 1979).

*Flagellar apparatus, striated collars, and peduncle:* The two slightly overlapping flagellar basal bodies were inserted at an angle of $\sim$100° with respect to each other (Fig. 5, F and G). A typical complement of flagellar roots was associated with the basal bodies. Thus, a microtubular root ($r_1$) consisting of 16 microtubules was associated with the left side of the longitudinal basal body (LB) (Figs. 5, E–G; 6, A–E), and the $r_2$ root comprising one microtubule embedded in a dense fiber was situated on the right ventral side of the LB (Figs. 5, E–G; 6, D and E). Two roots, $r_3$ and $r_4$, were attached to the right
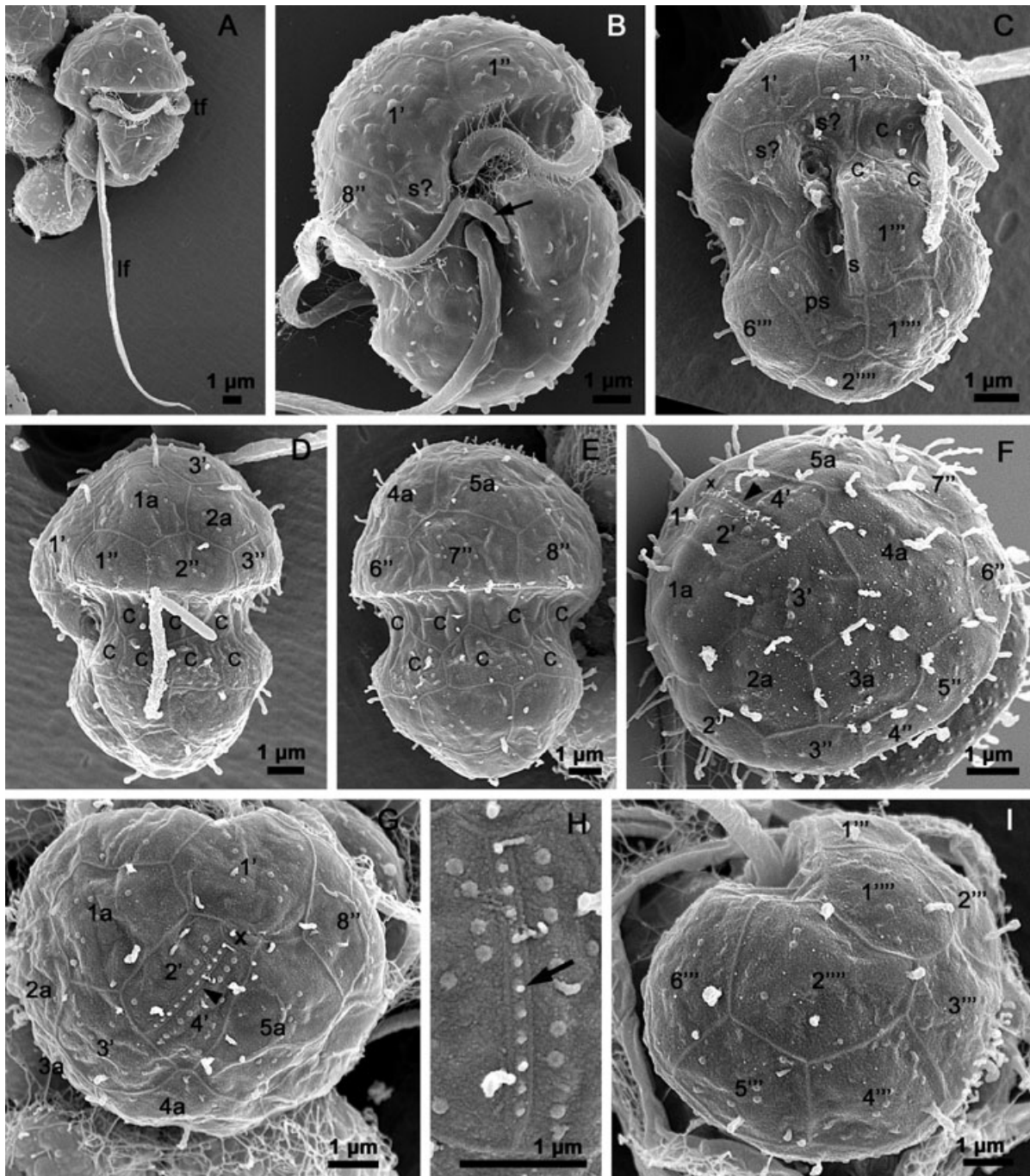
FIG. 2. *Symbiodinium natans* sp. nov., SEM, motile cells. (A) Cell displaying the transverse (tf) and longitudinal flagella (lf). (B) Cell in ventral view with intact flagella and a partly protruded peduncle (arrow). Some of the visible plates have been labeled. (C) Cell with discarded flagella and more clear plate pattern (ventral view). (D, E) Cells seen in left and right lateral views, respectively. (F) Episome seen in dorsal view; EAV-plate (arrowhead). (G) Episome seen in apical view. (H) The EAV plate in higher magnification. Notice the small knobs (arrow). (I) Antapical view of the hyposome.

dorsal and left side of the transverse basal body, respectively. The former consisted of a single microtubule that nucleated numerous microtubules (TMRE) (Fig. 5, C–G), the latter was a compound root consisting of a striated fiber (Figs. 5, E–G; 6, H and I) and a single microtubule (not shown). Several fibers interconnected the various components of the flagellar apparatus. The two basal bodies were connected by a small striated connective, the bbc (Fig. 5, E–G). The $r_1$ root was attached to the LB by two small fibers, the C1LB/$r_1$ and C2LB/$r_1$ (Fig. 6E), and to the TB by a small striated fiber,
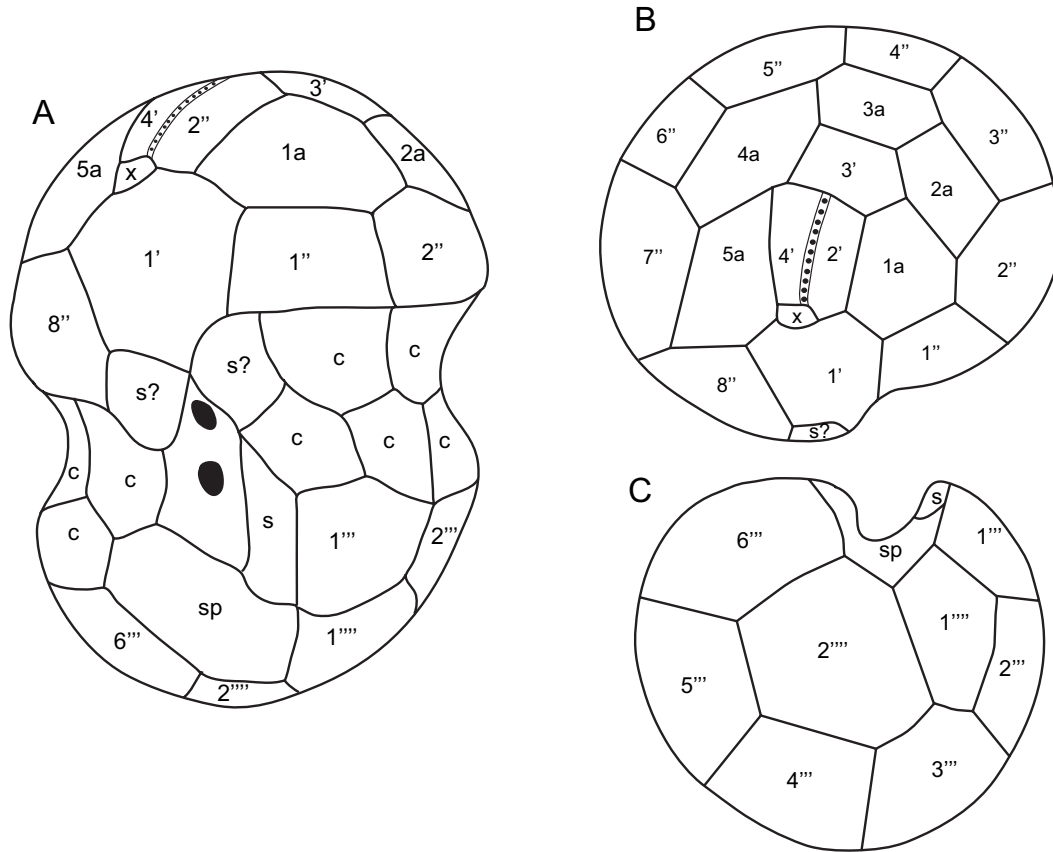
FIG. 3. The thecal plate pattern of *Symbiodinium natans* sp. nov. based on a compilation of SEM micrographs. (A) Ventral view. (B) Apical view. (C) Antapical view.

the $r_1/TBc$ (Figs. 5, E–G; 6G). The $r_1$ and $r_4$ roots were interlinked by a striated fiber, the src (Fig. 5, F and G). A dense fiber was situated on the right dorsal side of the $r_1$ root (Figs. 6, B–E).

Two dense collars or sphincters encircled each of the flagellar canals, the longitudinal (LSC) and transverse striated collar (TSC), although the striation was not apparent (Figs. 5, A, B, and E–G; 6, A–C; G–I). The two collars were interlinked by a dense fiber, probably representing the ventral ridge fiber (Figs. 5, B and C; 6, B–F). A ventral connective (vc) originating from the $r_1$ flagellar root attached to the ventral ridge and the LSC (Figs. 5F; 6, C and D).

The peduncle consisted of a microtubular strand terminating in electron dense fibrous material that seemed to represent part of the ventral ridge. It is likely that this material represented a closed sphincter similar to the LSC and TSC. Numerous electron dense bodies were situated in the vicinity of the microtubular strand (Fig. 5, A–B).

*Phylogeny.* Figure 7 illustrates the phylogeny deduced from BA, including 106 *Symbiodinium* LSU rDNA sequences and two outgroup taxa (i.e., *Gymnodinium beii* and *G. simplex*). The tree topology for clade A to H was consistent with Garcia-Cuetos

et al. (2005), and similar to this study, our analyses did not reveal details of the relationship between clades G, D, and the cluster that comprised clades B, F, H, and C, formed a trichotomy. Clade A branched at the base of the tree forming a sister clade to the remaining *Symbiodinium* clades (B to H). The individual clades designated A–E and G–H were highly supported in terms of posterior probabilities and bootstrap values from NJ analyses (1.0 = 100% in BA and ≥91% in NJ; Fig 7). Clade F received little bootstrap support from NJ analysis (54%) but high posterior probability (94%) from BA. *S. natans* clustered with 14 *Symbiodinium* LSU rDNA sequences assigned to clade A. Clade A was originally described more than 16 years ago (Rowan and Powers 1991). For reasons of comparison, we have divided clade A into four subclades, viz. $A_I$ (=temperate A, sensu Visram et al. 2006 but including a ribotype from eastern Australia, DQ060760), $A_{II}$ (=*Symbiodinium pilosum* and an unnamed Jamaican isolate, AF427456), $A_{III}$ (=*S. natans*), and $A_{IV}$ (=*Symbiodinium* from a diverge assemblage of Cnidaria host species sampled in tropical waters worldwide). Within clade A, subclade $A_I$ diverged first followed by subclade $A_{II}$. *S. natans* formed its own lineage (subclade $A_{III}$) and thus took a somewhat
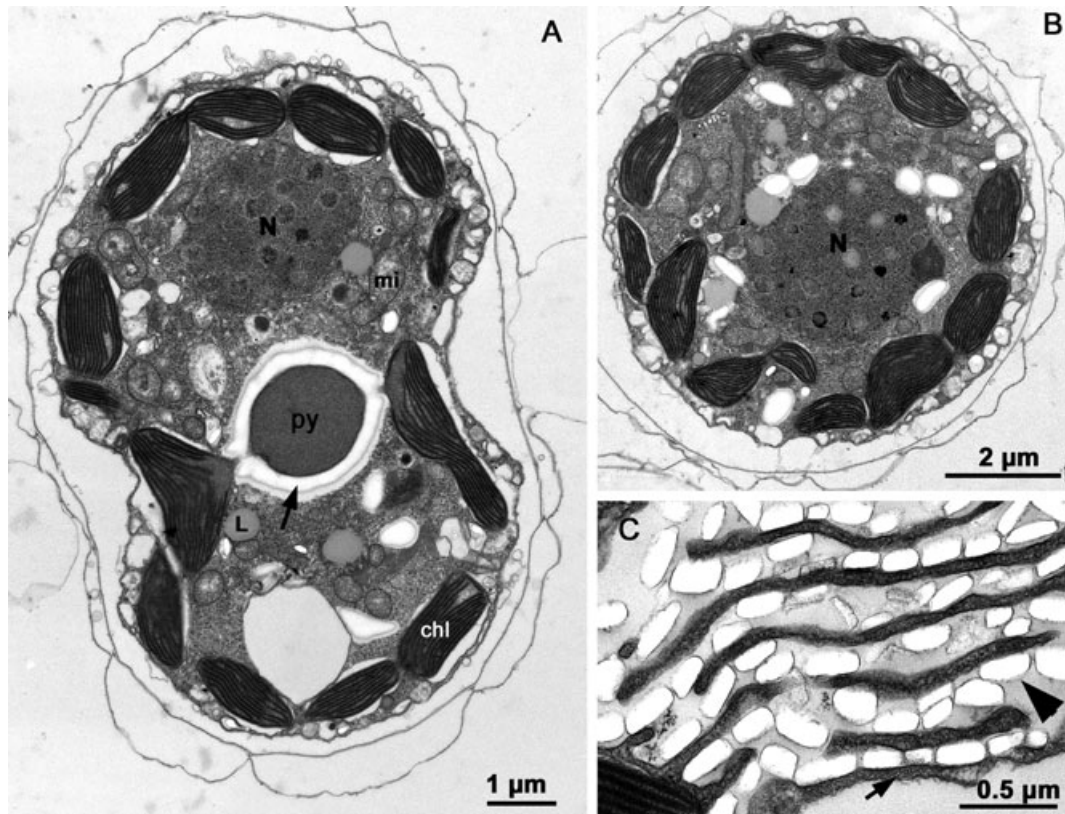
FIG. 4. *Symbiodinium natans* sp. nov., TEM, general ultrastructure. (A) Longitudinal section. N, nucleus; chl, chloroplast; py, pyrenoid; mi, mitochondrion; L, lipid droplet. Notice starch cap around the pyrenoid (arrow). (B) Transverse section. Notice peripheral location of chloroplasts. (C) The eyespot consisting of brick-containing cisternae (arrowhead). Notice microtubular strand (arrow).

isolated position. Subclade $A_{III}$ formed a sister taxon to subclade $A_{IV}$, which contained two isolates identified as *S. microadriaticum* in addition to many unidentified taxa. BA provided high posterior probabilities for the major branches of subclades in clade A ($\geq 92\%$), whereas NJ bootstrap values only provided high support for $A_I$ and $A_{II}$ (100% and 96%, respectively; Fig. 7). In NJ bootstrap analysis, the position of subclade $A_{II}$ and $A_{III}$ was switched compared to the topology shown in Figure 7. Otherwise, the resulting tree topologies were almost identical.

*Divergence estimates of subclades in clade A.* Table 1 shows divergence estimates for all pair-wise comparisons within subclades (intracladal divergence) and among subclades (intercladal divergence) of clade A comprising *S. natans*. The divergence estimates are based on 520 base pairs including the highly divergent domain D2 of the LSU rDNA gene. The intracladal divergence suggested by Bayesian phylogeny (Fig. 7) ranged from a few substitutions ($\leq 6$ base pair differences within subclades $A_I$ and $A_{II}$) up to 11 substitutions for subclade $A_{IV}$ (range 1–11). Thus, subclade $A_{IV}$ is the most diverse, and future morphological studies of motile cells are likely to recognize more species than the currently identified *S. microadriaticum*. The intercladal comparison

revealed that the sequence of *S. natans* is most divergent to subclades $A_I$ and $A_{II}$ (43–46 substitutions (=8.9%–9.5%) and 21–23 substitutions (=4.2%–4.6%), respectively). Interestingly, the intercladal sequence divergence estimates between subclades $A_{III}$ (=*S. natans*) and $A_{IV}$ is only slightly higher than the intracladal differences of subclade $A_{IV}$ (1.8%–2.8% and 0.2%–2.2%, respectively), indicating that these *Symbiodinium* taxa are more closely related and probably diverged more recently.

## DISCUSSSION

*Identity of the species.* Previously, the plate tabulation had only been analyzed in two strains of *S. microadriaticum,* one isolated from decaying *Chondus crispu*s Stackh. and one isolated from *Cassiopea* sp. The free-living and in hospite strain had essentially a similar plate arrangement (Loeblich and Sherley 1979), although the variations in tabulation given for the free-living and the symbiotic strain were 1 pr, 5′, 5a–6a, 9–10″, ca. 20c, 8–9s, 7–8‴, 3⁗ and 1 pr, 5′, 4a–6a, 10–11″, ca. 20c, 8–9s, 7–8‴, 3⁗, respectively. The plate arrangement of *S. natans* is very similar to *S. microadriaticum,* but with some significant differences. For example, *S. natans* has two rather than three antapical plates and only six
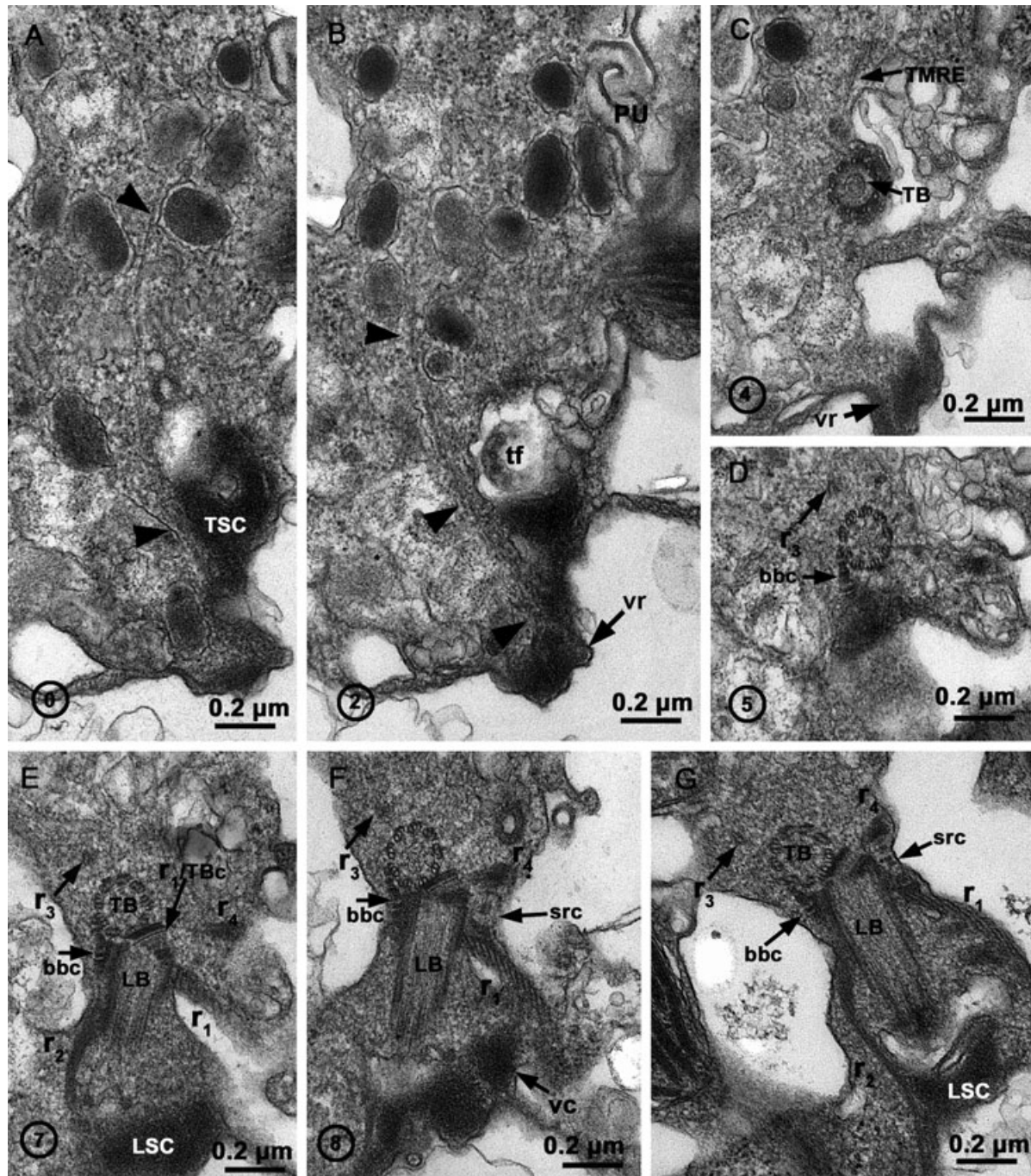
FIG. 5. *Symbiodinium natans* sp. nov., TEM. The flagellar apparatus in longitudinal view. (A–F) Nonadjacent serial sections. The cell is seen from the outside, and the sections are moving from ventral to dorsal. The encircled numbers are section numbers. (A, B) The microtubular strand of the peduncle with associated dense bodies (arrowheads) terminating at ventral ridge fiber (vr). TSC, transverse striated collar; PU, pusule. (C) Faint traces of the microtubular extension of the $r_3$ flagellar root (TMRE). TB: transverse basal body. (D–F) Sections showing the $r_1$, $r_2$, $r_3$, and $r_4$ flagellar roots and the connectives: bbc (basal body connective), $r_1$/TBc, connective between $r_1$ and TB, src (striated root connective) and vc (ventral connective) linking $r_1$ with the ventral ridge and longitudinal striated collar (LSC). LB, longitudinal basal body. (G) Section of another cell more clearly showing the $r_2$ root.

postcingular plates compared to the seven to eight postcingular plates in *S. microadriaticum.* Furthermore, the number of apical plates is only four in *S. natans* but five in *S. microadriaticum.* Particularly, the differences in the hyposomal plate pattern are noteworthy. Apart from the cingular and sulcal plates, the hyposomal plates are considered the most stable and conservative (Balech 1980). These differences alone justify *S. natans* as different from *S. microadriaticum* sensu Loeblich and Sherley.
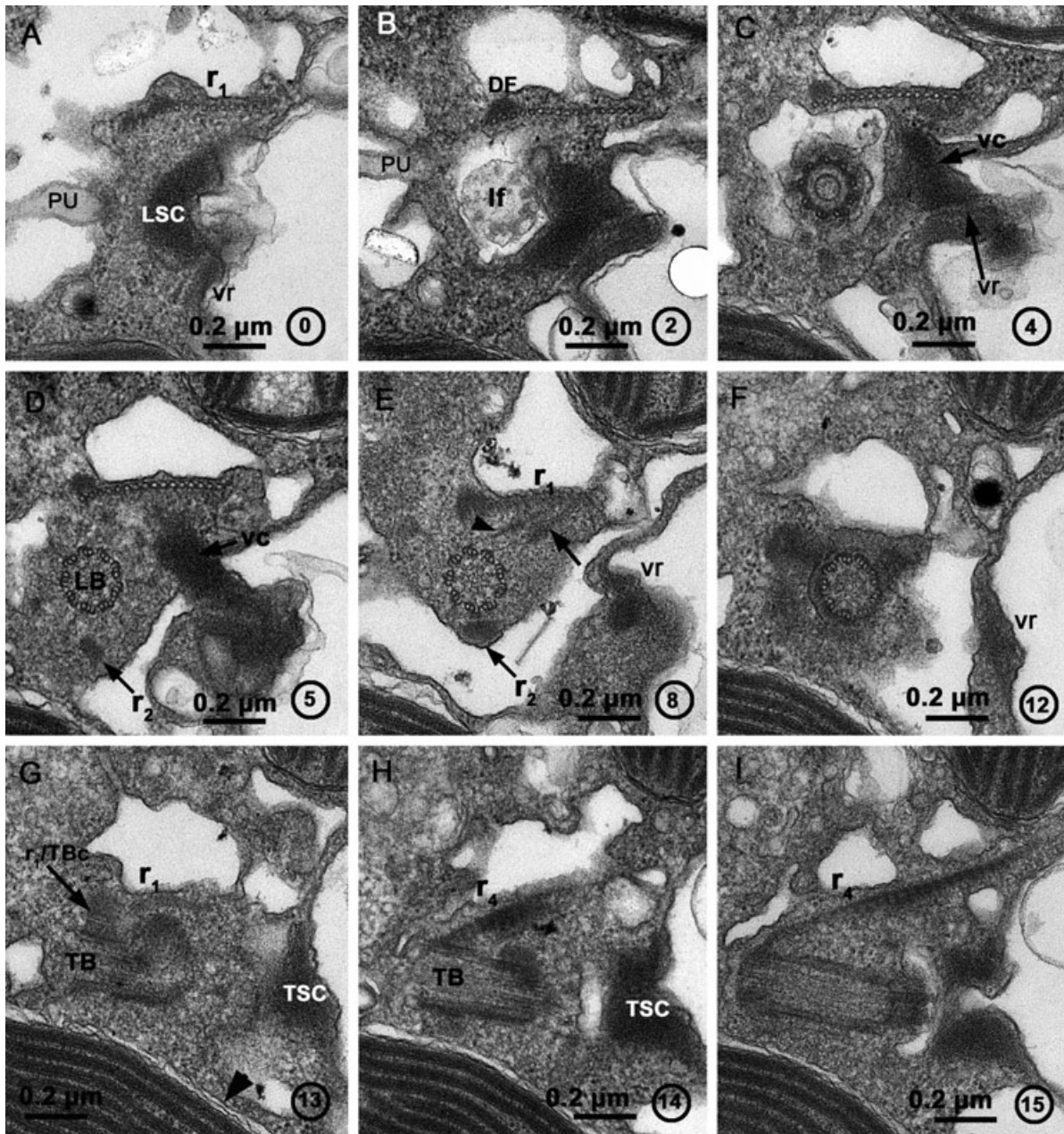
FIG. 6. *Symbiodinium natans* sp. nov., TEM. The flagellar apparatus in transverse view. (A–I) Nonadjacent serial sections. The cell is seen from the outside, and the sections are moving from posterior to anterior. The encircled numbers are section numbers. (A) Section at the level of the LSC with attached vr. Part of the PU is also visible. (B) A dorsal fiber (DF) is associated with the $r_1$ root. (C, D) The ventral connective (vc) is attached to the R1 root, the vr, and probably also LSC. Notice also the $r_2$ root imbedded in dense material. (E) Two small connectives link $r_1$ to the LB, the C1LB/$r_1$ (arrowhead) and C2LB/$r_1$ (arrow). (F) The proximal part of the LB. (G) The $r_1$/TBc. Notice also three chloroplast membranes (arrowhead). (H, I) The striated fiber of the $r_4$ flagellar root.

Additional differences are the episomal nucleus and displaced cingulum in *S. natans* compared to the hyposomal nucleus and nondisplaced cingulum in *S. microadriaticum* (Freudenthal 1962). Our phylogenetic analyses (Fig. 7) and sequence divergence estimates (Table 1) based on partial LSU sequences confirmed *S. natans* as separate from *S. microadriaticum*, but also from *S. pilosum* and *S. linucheae*, all belonging to clade A. The two other validly

described species, *S. goreauii* and *S. kawagutii*, are not included in the present analysis due to lack of sequence data available (<25 base pairs) but belong to clade C and F, respectively (Baker 2003). Thus, molecular data also confirmed *S. natans* as a new species.

The rather different hyposomal plate pattern of *S. natans* and *S. microadriaticum*, irrespective of the fact that both species belong to clade A is somewhat

AF060900 - [Orbulina universa] - 'Gymnodinium beii'
AF060901 - 'Gymnodinium simplex' (CCMP 420)

AJ830927 [Sorites sp.]
AJ830928 [Marginopora vertebralis]
AJ830929 [Marginopora vertebralis]
AJ620942 [Sorites sp.]
AJ311941 [Favites sp.]
AJ620935 [Sorites sp.]
AJ620937 [Sorites sp.]
AJ620945 [Sorites sp.]
AJ308889 [Pavona divaricata]
100 AJ830930 [Amphisorus hemprichii]
100 AJ621128 [Sorites sp.]
AJ311942 [Acropora sp.]
AJ278598 [Maristentor marianus]
AJ308891 [Oulaphyllia crispa]
100/91 AJ830897 [Marginopora kudakajimaensis]
AJ830899 [Marginopora kudakajimaensis]
AJ830931 [Sorites sp.]
C
AJ830901 [Amphisorus hemprichii]
100 AJ830902 [Marginopora vertebralis]
74 AJ830903 [Marginopora vertebralis]
100/ AJ291516 [Sorites sp.]
60 AJ311944 [Porites rus]
AJ830904 [Sorites sp.]
85/56 AJ291513 [Sorites sp.]
AJ621157 [Sorites sp.]
AJ830906 [Sorites sp.]
100 AJ291520 [Sorites sp.]
91 AJ621148 [Sorites sp.]
AJ621129 [Sorites sp.]
AJ621131 [Sorites sp.]
H
86/61 AJ621149 [Sorites sp.]
AJ621130 [Sorites sp.]
AJ621150 [Sorites sp.]

99/- 100 AJ830908 [Sorites sp.]
100 AJ830909 [Sorites sp.]
AJ830911 [Sorites sp.]
95/- AJ830913 [Unid. soritid]
85/100 69/- 100/100 AJ830912 [Unid. soritid]
100 AJ830916 [Amphisorus hemprichii]
99 AJ830915 [Amphisorus hemprichii]
58/- AJ308895 [Marginopora kudakajimaensis]
81 96/99 AJ291525 [Marginopora sp.]
AJ830917 [Amphisorus hemprichii]
91/96 AJ291535 [Sorites sp.]
AJ830918 [Amphisorus hemprichii]
100/100 AJ830919 [Sorites sp.]
84/- AJ830920 [Amphisorus hemprichii]
93/- AJ291512 [Sorites sp.]
94 AJ830922 [Amphisorus hemprichii]
54 100/99 AJ830924 [Sorites sp.]
AJ830925 [Amphisorus hemprichii]
F
AJ311949 [Sorites sp.]
54/87 AJ621137 [Sorites sp.]
AJ621135 [Sorites sp.]
100/100 AJ621136 [Sorites sp.]
100 AJ621142 [Sorites sp.]
AJ621145 [Sorites sp.]
100 AJ621139 [Sorites sp.]
AJ291527 [Sorites sp.]
100/100 AJ291528 [Sorites sp.]
AJ621147 [Sorites sp.]

100 97/- U63484 [Aiptasia pallida]
100 AF060892 Symbiodinium pulchrorum (clone 8)
AY074961 [Madracis mirabilis]
AY074960 [Meandrina meandrites]
AY074955 [Diploria labyrinthiformis]
81/- AY074946 [Favia fragum]
88/- DQ200694 [Montastraea annularis]
DQ200703 [Montastraea annularis]
100 AY074972 [Diploria strigosa]
100 AY074962 [Montastraea franksi]
AY074966 [Montastraea annularis]
AY074958 [Isophyllia sinuosa]
AF060891 Symbiodinium bermudense
B

100 100 AJ830923 [Marginopora vertebralis]
100 AJ308899 [Haliclona koremella]
100 AJ308900 [Pavona decusata]
93 AY903350 Symbiodinium sp. (clone PdSing3)
AJ308902 [Acropora palifera]
AJ308901 [Goniopora fruticosa]
100 AJ311948 [Acropora sp.]
100 AB280701 Symbiodinium sp. (clone SC13.2)
AY588445 [Galaxea fascicularis]
AF396626 [Acropora sp.]
AY074951 [Siderastrea siderea]
AY074957 [Goniastrea aspera]
D

100 97 100 98 69/71 100 AJ291537 [Amphisorus sp.]
100 AJ291536 [Marginopora sp.]
100 AJ291539 [Amphisorus sp.]
AJ291538 - [Marginopora vertebralis]
G
E

100 100 AF060899 - 'Gymnodinium varians'
U63483 Symbiodinium microadriaticum
100/- AF060896 Symbiodinium microadriaticum (clone 61)
AJ311946 [Millepora sp.]
99/- AF060893 Symbiodinium linucheae
100/66 AY074968 [Porites porites]
55/- AY074967 [Porites astreoides]
92/- DQ981495 [Acropora longicyathus]
AY074953 [Stephanocoenia intersepta]
A_{IV}
100/- EU315917 Symbiodinium natans sp. nov.
A_{III}
100 AF060894 Symbiodinium pilosum
96 AF427456 [Zoanthus sociatus]
A_{II}
AY074939 [Anemonia viridis]
100 DQ060760 [Tridacna maxima]
100 AY074975 [Anemonia sulcata var. vulgaris]
AY588464 [Cribinopsis crassa]
A_{I} (=temperate A)
A

0.1

TABLE 1. Comparison in absolute number of differences and divergence estimates based on the Kimura-2-Parameter model using PAUP* (ver. 4b10) based on 520 unambiguously aligned base pairs of LSU rDNA sequences. See Figure 7 for definition of subclades $A_I$ to $A_{IV}$.

| Subclades $A_I$ to $A_{IV}$ | Range of absolute number of differences | Range of divergence estimates based on Kimura-2-P (%) |
|---|---|---|
| $A_I$–$A_I$ | 1–6 | 0.2–1.2 |
| $A_I$–$A_{II}$ | 52–57 | 11.0–12.1 |
| $A_I$–$A_{III}$ | 43–46 | 8.9–9.5 |
| $A_I$–$A_{IV}$ | 47–56 | 9.6–11.9 |
| $A_{II}$–$A_{II}$ | 2 | 0.4 |
| $A_{II}$–$A_{III}$ | 21–23 | 4.2–4.6 |
| $A_{II}$–$A_{IV}$ | 24–29 | 4.8–5.9 |
| $A_{III}$–$A_{III}$ | – | – |
| $A_{III}$–$A_{IV}$ | 9–14 | 1.8–2.8 |
| $A_{IV}$–$A_{IV}$ | 1–11 | 0.2–2.2 |

puzzling. The plate pattern of species within other clades is unknown, but such differences would be expected to reflect inter- rather than intracladal differences.

*Ultrastructure and phylogeny of* Symbiodinium. Recent studies have shown that *Symbiodinium* together with *Polarella glacialis* Montresor, Procaccini et Stoecker, *Woloszynskia halophila* (Biecheler) Elbr. et Kremp, and *W. pseudopalustris* (J. Schiller) Kisselev constitute a well-supported clade (Kremp et al. 2005, Moestrup et al. 2008). The ultrastructural feature uniting these groups is the peculiar eyespot consisting of cisternae with brick-shaped contents, type E eyespot sensu Moestrup and Daugbjerg (2007). This type of eyespot was also a very conspicuous feature in *S. natans* and had previously been observed in *Symbiodinium linucheae* (Trench and Thinh 1995, as *Gymnodinium linucheae*), although misinterpreted as a microtubular basket. It is likely that *Prosoaulax lacustre* (F. Stein) Calado et Moestrup and *Gymnodinium natalense* T. Horig. et Pienaar also belong to this clade, as they too have a type E eyespots (Horiguchi and Pienaar 1994, Calado et al. 1998, Calado and Moestrup 2005).

Another feature shared by *Symbiodinium*, *W. halophila*, *W. pseudopalustris,* and *P. lacustre* is the apical structure, consisting of a single narrow elongated plate or vesicle the EAV (Moestrup and Daugbjerg 2007). *Polarella glacialis* lacks an apical structure, which is consistent with the LSU phylogeny of Kremp et al. (2005), revealing *P. glacialis* as a sister

taxon to *Symbiodinium*, *W. halophila,* and *W. pseudopalustris*, but contradictory with the recent phylogenies in Moestrup and Daugbjerg (2007) and Moestrup et al. (2008) showing *Symbiodinium* rather than *P. glacialis* as the sister taxon. The recently erected genus *Borghiella*, which together with *Baldinia anauniensis* Gert Hansen et Daugbjerg forms a sister group to the above mentioned clade, has a very similar apical structure but consists of two rather than one amphiesmal vesicle, the PEV (pair of elongated amphiesmal vesicles) sensu Moestrup et al. (2008). Interestingly, *B. anauniensis*, like *P. glacialis*, lacks an apical structure.

The flagellar apparatus of *Symbiodinium* consists of typical dinoflagellate components, that is, $r_1$–$r_4$ flagellar roots and fibrous collars around the flagellar canals. It is basically similar to that described for *Borghiella dodgei* Moestrup, Gert Hansen et Daugbjerg, with respect to the various connectives interlinking the flagellar roots and the basal bodies, with one notable difference, the presence of a ''hub-spoke'' structure around the basal bodies in *B. dodgei* (Moestrup et al. 2008). A structure previously only observed in *Jadwigia applanata* Moestrup, K. Lindb. et Daugbjerg (Roberts et al. 1995, as *W. limnetica* Bursa) and *Woloszynskia pascheri* (Suchl.) Stosch sensu Wilcox (1989). The flagellar apparatus of *B. anauniensis* differs from *Symbiodinium* and *Borghiella* by the presence of a ventral fiber, an incomplete longitudinal striated collar, and a peculiar lamellar body surrounding the basal bodies (Hansen et al. 2007). Loeblich and Sherley (1979) observed a projection between emergence points of the two flagella in *Symbiodinium microadriaticum* and considered it to be a peduncle. Thin section TEM of *S. natans* confirms that *Symbiodinium* has a peduncle similar to that observed in a many dinoflagellates. It is not the microtubular basket type present in, for example, *Gyrodinium lebouriae* Herdmann (Lee 1977) and *Paulsenella* sp. (Schnepf et al. 1985), but the more common type consisting of a single microtubular strand. Its function is puzzling as it is hardly used for food uptake in an organism living as an endosymbiont presumably for most of its life history. Loeblich and Sherley (1979) suggested it to be used for attachment, due to the rapid spinning behavior of the motile cell indicating attachment to the substrate. However, if *S. natans* is truly free living, the peduncle might be used for food uptake. For example, *B. anauniensis* also has a peduncle, and

FIG. 7. Phylogeny of *Symbiodinium natnas* sp. nov. based on 815 base pairs of the nuclear-encoded LSU rDNA gene (corresponding to domain D1 and D2 sensu Lenaers et al. 1989). The tree topology illustrated is from a Bayesian analysis, and the branch lengths are proportional to the amount of character changes. The alignment included an additional 105 rDNA *Symbiodinium* sequences representing the previously defined clades A to H; these are labeled to the right. Homologous LSU rDNA sequences of *Gymnodinium beii* and *G. simplex* were used to polarize the *Symbiodinium* ingroup. Posterior probabilities from Bayesian analyses and bootstrap values (1,000 replications) from neighbor-joining (NJ) analyses are written to the left of internal nodes. Values below 50% are indicated as ''–''. GenBank accession numbers are provided for each operational taxonomic unit. Names in square brackets indicate either the invertebrate host or the foraminiferan species from which the *Symbiodinium* sequences were obtained. Free-living *Symbiodinium* species are indicated with their formal and informal names. The LSU rDNA sequence from *S. natans* determined in this study is boldfaced. For reasons of comparison, the earliest diverging clade A has been divided into four subclades labeled $A_I$ to $A_{IV}$ (see also text). Please note that the four subclades have been labeled as to distinguish them from those defined by LaJeunesse (2001).

this species is mixotrophic feeding on, for example, small cryptophytes (Hansen et al. 2007). Interestingly, *B. dodgei* lacks a peduncle (Moestrup et al. 2008).

It is clear that several features separate the clade comprising *Polarella*, *Symbiodinium*, *Woloszynskia halophila,* and *W. pseudopalustris* from the clade comprising *Baldinia* and *Borghiella*. However, it is less obvious what morphological characters link these groups into a major clade, apart from the fact that all species lack trichocysts and possess two rows of cingular plates (Montresor et al. 1999, Kremp et al. 2005, Moestrup et al. 2008).

An interesting question is whether the free-living stage of *S. natans* is permanent or merely a temporary motile stage awaiting the right host. Its phylogenetic position within clade A does not suggest any obvious hosts. However, clade A in the present analysis primarily consists of *Symbiodinium* spp. within cnidarians, but a non-cnidarian host cannot be excluded. Studies based on free-living strains of *Symbiodinium* are rare, and their infection potential, if any, remains largely unknown (Loeblich and Sherley 1979, Carlos et al. 1999, Gou et al. 2003). However, a recent study based on several strains of free-living *Symbiodinium* from Florida Keys, showed these were able to infect cnidarian recruits, although some strains belonging to clade A appeared to be noninfectious (Coffroth et al. 2006). Due to the unfortunate breakdown of our culture cabinet resulting in the death of *S. natans*, studying of its infection potential is currently not possible.

In conclusion, the present study has indicated the potential application of plate tabulation for the taxonomy of *Symbiodinium*. Details of the plate arrangement have only been made on two species, and therefore more species from different clades (e.g., B to H) need to be analyzed before an evident evaluation of inter- and intracladel plate variation can be undertaken. However, in an attempt to improve our understanding of species distribution of *Symbiodinium* on a local and regional scale, we propose to combine information from molecular methods with observations of plate tabulation characteristics.

Baker, A. C. 2003. Flexibility and specificity in coral-algal symbiosis: diversity, ecology, and biogeography of *Symbiodinium*. *Annu. Rev. Ecol. Evol. Syst.* 34:661–89.

Balech, E. 1980. On the thecal morphology of dinoflagellates with special emphasis on cingular and sulcal plates. *An. Centro del Mar Limnol. Univ. Nal. Autón. Mexico* 7:57–68.

Banaszak, A. T., Iglesias-Prieto, R. & Trench, R. K. 1993. *Scrippsiella velellae*, sp. nov. (Peridiniales) and *Gloeodinium viscum*, sp. nov. (Phytodiniales) dinoflagellate symbionts of two hydrozoans (Cnidaria). *J. Phycol.* 29:517–28.

Calado, A. J., Craveiro, S. C. & Moestrup, Ø. 1998. Taxonomy and ultrastructure of a freshwater, heterotrophic *Amphidinium* (Dinophyceae) that feeds on unicellular protists. *J. Phycol.* 34:536–54.

Calado, A. J. & Moestrup, Ø. 2005. On the freshwater dinoflagellates presently included in the genus *Amphidinium*, with a description of *Prosoaulax* gen. nov. *Phycologia* 44:112–19.

Carlos, A. A., Baillie, B., Kawachi, M. & Maruyama, T. 1999. Phylogenetic position of *Symbiodinium* (Dinophyceae) isolates from tridacnids (Bivalvia), cardiids (Bivalvia), a sponge (Porifera), a soft coral (Anthozoa), and a free-living strain. *J. Phycol.* 35:1054–62.

Coffroth, M. A., Lewis, C. F., Santos, S. R. & Weaver, J. L. 2006. Environmental populations of symbiotic dinoflagellates in the genus *Symbiodinium* can initiate symbioses with reef cnidarians. *Curr. Biol.* 16:R985–7.

Coffroth, M. A. & Santos, S. R. 2005. Genetic diversity of symbiotic dinoflagellates in the genus *Symbiodinium*. *Protist* 156:19–34.

Daugbjerg, N., Hansen, G., Larsen, J. & Moestrup, Ø. 2000. Phylogeny of some of the major genera of dinoflagellates based on ultrastructure and partial LSU rDNA sequence data, including the erection of three new genera of unarmoured dinoflagellates. *Phycologia* 39:302–17.

Daugbjerg, N., Moestrup, Ø. & Arctander, P. 1994. Phylogeny of the genus *Pyramimonas* (Prasinophyceae) inferred from the *rbc*L gene. *J. Phycol.* 30:991–9.

Dodge, J. D. 1967. Fine structure of the dinoflagellate *Aureodinium pigmentosum* gen. et sp. nov. *Br. Phycol. Bull.* 3:327–36.

Fensome, R. A., Taylor, F. J. R., Norris, G., Sarjeant, W. A. S., Wharton, D. I. & Williams, G. L. 1993. *A Classification of Living and Fossil Dinoflagellates*. Micropaleontology special publication number 7. American Museum of Natural History, Salem, Massachusetts, 351 pp.

Freudenthal, H. D. 1962. *Symbiodinium* gen. nov. and *Symbiodinium microadriaticum* sp. nov; a zooxanthella: taxonomy, life cycle and morphology. *J. Protozool.* 9:45–52.

Garcia-Cuetos, L., Pochon, X. & Pawlowski, J. 2005. Molecular evidence for host-symbiont specificity in soritid foraminifera. *Protist* 156:399–412.

Gast, R. J. & Caron, D. A. 1996. Molecular phylogeny of symbiotic dinoflagellates from planktonic Foraminifera and Radiolaria. *Mol. Biol. Evol.* 13:1192–7.

Gou, W., Sun, J., Li, X., Zhen, Y., Xin, Z., Yu, Z. & Li, R. 2003. Phylogenetic analysis of a free-living strain of *Symbiodinium* isolated from Jiaozhou Bay, P.R. *China. J. Exp. Mar. Biol. Ecol.* 296:135–44.

Hansen, G., Daugbjerg, N. & Henriksen, P. 2007. *Baldinia anauniensis* gen. et sp. nov. a 'new' dinoflagellate from Lake Tovel. *Phycologia* 46:86–108.

Horiguchi, T. & Pienaar, R. N. 1994. *Gymnodinium natalense* sp. nov. (Dinophyceae), a new tide pool dinoflagellate from South Africa. *Jpn. J. Phycol.* 42:21–8.

Kremp, A., Elbrächter, M., Schweikert, M., Wolny, J. L. & Gottschling, M. 2005. *Woloszynskia halophila* (Biecheler) comb. nov.: a bloom-forming cold-water dinoflagellate co-occurring with *Scrippsiella hangoei* (Dinophyceae) in the Baltic Sea. *J. Phycol.* 41:629–42.

LaJeunesse, T. C. 2001. Investigating the biodiversity, ecology, and phylogeny of endosymbiotic dinoflagellates in the genus *Symbiodinium* using the ITS region: in search of a ''species'' level marker. *J. Phycol.* 37:866–80.

LaJeunesse, T. C. & Trench, R. K. 2000. Biogeography of two species of *Symbiodinium* (Freudenthal) inhabiting the intertidal sea anemone *Anthopleura elegantissima* (Brandt). *Biol. Bull.* 199:126–34.

Larsen, N. H., Moestrup, Ø. & Pedersen, P. M. 1994. *Scandinavian Culture Centre for Algae & Protozoa. Catalogue*. Department of Phycology, University of Copenhagen, Copenhagen, Denmark, 51 pp.

Lee, R. E. 1977. Saprophytic and phagocytic isolates of the colorless heterotrophic dinoflagellate *Gyrodinium lebouriae* Herdman. *J. Mar. Biol. Assoc. U. K.* 57:303–15.

Lenaers, G., Maroteaux, L., Michot, B. & Herzog, M. 1989. Dinoflagellates in evolution. A molecular phylogenetic analysis of large subunit ribosomal RNA. *J. Mol. Evol.* 29:40–51.

Loeblich, A. R. III. & Sherley, J. L. 1979. Observations on the theca of the motile phase of free-living and symbiotic isolates of *Zooxanthella microadriatica* (Freudenthal) comb. nov. *J. Mar. Biol. Assoc. U. K.* 59:195–205.

Maddison, D. R. & Maddison, W. P. 2003. *MacClade 4.* Sinauer Associates Inc., Sunderland, Massachusetts.

McLaughlin, J. J A & Zahl, P. A. 1966. Endozoic algae. *In* Henry, S. M. [Ed.] *Symbiosis. Vol. I. Associations of Microorganisms, Plants, and Marine Organisms.* Academic Press, New York, pp. 257–97.

Moestrup, Ø. & Daugbjerg, N. 2007. On dinoflagellate phylogeny and classification. *In* Brodie, J. & Lewis, J. [Eds.] *Unravelling the Algae: The Past, Present, and Future of Algae Systematics.* Systematics Association Special Volumes, Vol. 75. CRC Press, Boca Raton, Florida, pp. 215–30.

Moestrup, Ø., Hansen, G. & Daugbjerg, N. 2008. Studies on woloszynskioid dinoflagellates III: on *Borghiella* gen. nov., and *B. dodgei* sp. nov., a cold-water species from Lago di Tovel, N. Italy, and on B. tenuissima comb. nov. (syn. *Woloszynskia tenuissima*). *Phycologia* 47:54–78.

Montresor, M., Procaccini, G. & Stoecker, D. K. 1999. *Polarella glacialis*, gen. nov., sp. nov. (Dinophyceae): Suessiaceae are still alive! *J. Phycol.* 35:186–97.

Nunn, G. B., Theisen, B., Christensen, B. & Arctander, P. 1996. Simplicity-correlated size growth of the nuclear 28S ribosomal RNA D3 expansion segment in the crustacean order isopoda. *J. Mol. Evol.* 42:211–23.

Pochon, X., Montoya-Burgos, J. I., Stadelmann, B. & Pawlowski, J. 2006. Molecular phylogeny, evolutionary rates, and divergence timing of the symbiotic dinoflagellate genus *Symbiodinium. Mol. Phylogenet. Evol.* 38:20–30.

Posada, D. & Crandall, K. A. 1998. Modeltest: testing the model of DNA substitution. *Bioinformatics* 14:817–18.

Roberts, K. R., Hansen, G. & Taylor, F. J. R. 1995. General ultrastructure and flagellar apparatus architecture of *Woloszynskia limnetica* (Dinophyceae). *J. Phycol.* 31:948–57.

Ronquist, F. & Huelsenbeck, J. P. 2003. MRBAYES 3: Bayesian phylogenetic inference under mixed models. *Bioinformatics* 19:1572–4.

Rowan, R. 1998. Diversity and ecology of zooxanthellae on coral reefs. *J. Phycol.* 34:407–17.

Rowan, R. & Powers, D. A. 1991. A molecular genetic classification of zooxanthellae and the evolution of animal-algal symbioses. *Science* 251:1348–51.

Rowan, R. & Powers, D. A. 1992. Ribosomal RNA sequences and the diversity of symbiotic dinoflagellates (zoozanthellae). *Proc. Natl. Acad. Sci. U. S. A.* 89:3639–43.

Santos, S. R., Taylor, D. J., Kinzie, R. A. III., Hidaka, M., Sakai, K. & Coffroth, M. A. 2002. Molecular phylogeny of symbiotic dinoflagellates inferred from partial chloroplast large subunit (23S)-rDNA sequences. *Mol. Phylogenet. Evol.* 23:97–111.

Schnepf, E., Deichgräber, G. & Drebes, G. 1985. Food uptake and the fine structure of *Paulsenella* sp., an ectoparasite of marine diatoms. *Protoplasma* 124:188–204.

Scholin, C. A., Herzog, M., Sogin, M. & Anderson, D. M. 1994. Identification of group-and strain-specific genetic markers for globally distributed *Alexandrium* (Dinophyceae). II. Sequence analysis of a fragment of the LSU rRNA gene. *J. Phycol.* 30:999–1011.

Swofford, D. L. 2003. *PAUP\* Phylogenetic Analysis Using Parsimony (\*and Other Methods), version 4.* Sinauer Associates, Sunderland, Massachusetts.

Tamura, K. & Nei, N. 1993. Estimation of the number of nucleotide substitutions in the control region of mitochondrial DNA in humans and chimpanzees. *Mol. Biol. Evol.* 10:512–26.

Trench, R. K. 1987. Dinoflagellates in non-parasitic symbioses. *In* Taylor, F. J. R. [Ed.] *The Biology of Dinoflagellates. Bot. Monographs,* Vol. 21. Blackwell Scientific Publications, Oxford, UK, pp. 530–70.

Trench, R. K & Blank, R. J. 1987. *Symbiodinium microadriaticum* Freudenthal; *S. goreauii* sp. nov; *S. kawagutii* sp. nov. and *S. pilosum* sp. nov.: gymnodinioid dinoflagellate symbionts of marine invertebrates. *J. Phycol.* 23:469–81.

Trench, R. K. & Thinh, L.-V. 1995. *Gymnodinium linucheae* sp. nov.: the dinoflagellate symbiont of the jellyfish *Linuche unguiculata. Eur. J. Phycol.* 30:149–54.

Visram, S., Wiedenmann, J. & Douglas, A. E. 2006. Molecular diversity of symbiotic algae of the genus *Symbiodinium* (Zooxanthellae) in cnidarians of the Mediterranean Sea. *J. Mar. Biol. Assoc. U. K.* 86:1281–3.

Wakefield, T. S., Farmer, M. A. & Kempf, S. C. 2000. Revised description of the fine structure of in situ ''Zooxanthellae'' genus *Symbiodinium. Biol. Bull.* 199:76–84.

Wilcox, L. W. 1989. Multilayered structures (MLSs) in two dinoflagellates, *Katodinium campylops* and *Woloszynskia pascheri. J. Phycol.* 25:785–9.

Wilcox, T. P. 1998. Large-subunit ribosomal RNA systematics of symbiotic dinoflagellates: morphology does not recapitulate phylogeny. *Mol. Phylogenet. Evol.* 10:436–48.

Wilgenbusch, J. C., Warren, D. L. & Swofford, D. L. 2004. *AWTY: A System for Graphical Exploration of MCMC Convergence in Bayesian Phylogenetic Inference.* Available at: http://ceb.csit.fsu.edu/awty (last accessed 22 November 2007).